slow microtubule sliding velocities in *pf*14*pf*28 are not due to the lack of inner arm heavy chain 3′.

We tested whether inner arm heavy chain 3′ was the activating factor by reconstituting *pf*14*pf*28 axonemes with inner arms from *pf*13A. The resulting sliding velocities were not significantly different from those obtained with extracts from *pf*28 axonemes (1.5 ± 0.3 μm/s, n = 14 in NaCl; 2.4 ± 0.7 μm/s, n = 29 in KCH_3COO). Because the only difference between *pf*13A and *pf*14*pf*28 is the presence or absence of spokes, our results with extracts from *pf*28 cannot be explained by the contribution of a subset of inner arms from *pf*28 axonemes.

Our interpretation is that the spokes activate the inner dynein arms by a modification that survives high salt extraction and dialysis required for reconstitution. [Certain inner arm subforms may be differentially affected (*20*).] This interpretation was supported by comparison of sliding velocities of other axonemes defective for radial spokes (those of *pf*14, *pf*1, *pf*17, and *pf*27) with wild-type axonemes (those of 137c). Axonemal microtubules from all of these mutants slid at one-half to one-third the velocity of wild-type microtubules in both buffer conditions (Table 2), indicating that reduced microtubule sliding velocities are not unique to the *pf*14 mutation and that the outer arms cannot overcome the inactivation caused by the lack of radial spokes. Outer dynein arm activity might also be affected by the spokes in wild-type axonemes, as suggested by an unusual class of suppressor mutants (*sup-pf*1) in which the requirement of radial spokes for movement is bypassed by a defect in the beta heavy chain of the outer dynein arms (*12*). Calculations of sliding velocities (*12*) and those measured from sliding disintegration (those of *pf*17, compared with those of *sup-pf*1*pf*17 and *sup-pf*1, Table 2) indicate that the suppressor mutation increases microtubule sliding velocities in the absence of the spokes. Our results indicate activation of dynein-induced microtubule sliding activity by the radial spokes.

REFERENCES AND NOTES

1. P. Satir, *J. Cell Biol.* **39**, 77 (1968).
2. K. E. Summers and I. R. Gibbons, *Proc. Natl. Acad. Sci. U.S.A.* **68**, 3092 (1971).
3. C. J. Brokaw, *Science* **243**, 1593 (1989).
4. G. S. Bloom, *Curr. Opin. Cell Biol.* **4**, 66 (1992).
5. G. B. Witman, *ibid.*, p. 77; K. A. Johnson, *Annu. Rev. Biophys. Biophys. Chem.* **14**, 161 (1985).
6. W. S. Sale and P. Satir, *Proc. Natl. Acad. Sci. U.S.A.* **74**, 2045 (1977); L. A. Fox and W. S. Sale, *J. Cell Biol.* **105**, 1781 (1987).
7. C. J. Brokaw, *J. Cell Biol.* **114**, 1201 (1991).
8. F. D. Warner and P. Satir, *ibid.* **63**, 35 (1974); C. Omoto and C. Kung, *ibid.* **87**, 33 (1980).
9. B. Huang, *Int. Rev. Cytol.* **99**, 181 (1986).
10. G. Piperno, B. Huang, Z. Ramanis, D. J. L. Luck, *J. Cell Biol.* **88**, 73 (1981); B. Huang, G. Piperno, Z. Ramanis, D. J. L. Luck, *ibid.*, p. 80.
11. D. Luck, G. Piperno, Z. Ramanis, B. Huang, *Proc. Natl. Acad. Sci. U.S.A.* **74**, 3456 (1977); D. R. Diener *et al.*, *ibid.* **87**, 5739 (1990).
12. B. Huang, Z. Ramanis, D. J. L. Luck, *Cell* **28**, 115 (1982); C. J. Brokaw, B. Huang, D. J. L. Luck, *J. Cell Biol.* **92**, 722 (1982); C. J. Brokaw and R. Kamiya, *Cell Motil. Cytoskeleton* **8**, 68 (1987).
13. D. J. L. Luck and G. Piperno, in *Cell Movement: The Dynein ATPases*, F. D. Warner, P. Satir, I. R. Gibbons, Eds. (Liss, New York, 1989), vol. 1, chap. 4.
14. G. B. Witman, J. Plummer, G. Sander, *J. Cell Biol.* **76**, 729 (1978).
15. Flagella were isolated by the dibucaine method and resuspended in a buffer containing 10 mM Hepes (pH 7.4), 5 mM $MgSO_4$, 1 mM dithiothreitol (DTT), 0.5 mM EDTA, and 30 mM NaCl (NaCl buffer) with 0.1 mM phenylmethylsulfonyl fluoride and 0.6 trypsin inhibitor unit aprotinin, 4°C, and remained in this buffer until sliding disintegration was performed with the methods of Okagaki and Kamiya (*16*), with modifications as described in (*19*). As Tables 1 and 2 indicate, sliding disintegration was also performed in a KCH_3COO buffer [30 mM Hepes (pH 7.4), 5 mM $MgSO_4$, 1 mM DTT, 1.0 mM EGTA, 50 mM KCH_3COO, and 0.5% polyethylene glycol] (*22*). Axonemes were prepared as above except that adherent axonemes were washed with KCH_3COO buffer and sliding was induced by perfusion with the KCH_3COO buffer containing 1 mM ATP and nagarose (1 to 2 μg/ml). All sliding disintegration was recorded on videotape with a silicone intensified target camera and dark-field microscopy as described in (*16*). Analysis was restricted to axonemes in which sliding between pairs of microtubules or pairs of microtubule groups could be distinguished. Performing sliding disintegration with extracted axonemes in reconstitution experiments did not require prior sonication. Sliding velocities were measured manually from the video screen.
16. T. Okagaki and R. Kamiya, *J. Cell Biol.* **103**, 1895 (1986).
17. C. J. Brokaw, *Science* **207**, 1365 (1980).
18. R. Kamiya, E. Kurimoto, H. Sakakibara, T. Okagaki, in (*13*), chap. 15.
19. E. F. Smith and W. S. Sale, *J. Cell Biol.* **117**, 573 (1992).
20. G. Piperno, Z. Ramanis, E. F. Smith, W. S. Sale, *ibid.* **110**, 379 (1990); G. Piperno and Z. Ramanis, *ibid.* **112**, 701 (1991).
21. G. Piperno and D. J. L. Luck, *Cell* **27**, 331 (1981).
22. E. Kurimoto and R. Kamiya, *Cell Motil. Cytoskeleton* **19**, 275 (1991).
23. E. Muto, R. Kamiya, S. Tsukita, *J. Cell Sci.* **99**, 57 (1991).

24. We thank G. Piperno for helpful discussion and for mutant strains of *Chlamydomonas*. Supported by NIH research grant HD 20497 and training grant GM 08367.

30 April 1992; accepted 9 July 1992

NMR Determination of Residual Structure in a Urea-Denatured Protein, the 434-Repressor

Dario Neri,* Martin Billeter, Gerhard Wider, Kurt Wüthrich†

A nuclear magnetic resonance (NMR) structure determination is reported for the polypeptide chain of a globular protein in strongly denaturing solution. Nuclear Overhauser effect (NOE) measurements with a 7 molar urea solution of the amino-terminal 63-residue domain of the 434-repressor and distance geometry calculations showed that the polypeptide segment 54 to 59 forms a hydrophobic cluster containing the side chains of Val^{54}, Val^{56}, Trp^{58}, and Leu^{59}. This residual structure in the urea-unfolded protein is related to the corresponding region of the native, folded protein by simple rearrangements of the residues 58 to 60. Based on these observations a model for the early phase of refolding of the 434-repressor(1-63) is proposed.

Investigations of proteins in strongly denaturing solution are of general interest relative to the protein folding problem (*1*, *2*). For example, strongly denaturing solutions are often used as the "random-coil" reference state in refolding studies, and residual nonrandom structure found under such conditions might be indicative of nucleation sites for the refolding process. Structure determinations of partially or fully unfolded polypeptides are intrinsically difficult, and structural data on such species are scarce. Here we use the NMR method that is now in widespread use for studies of native, folded proteins (*3*, *4*) for a structure determination of the urea-unfolded form of the amino-terminal 63-residue domain of the 434-repressor.

For a polypeptide consisting of the amino-terminal residues 1 to 69 of the 434-repressor, which includes the DNA-binding domain (*5*), the three-dimensional structure has been determined at high resolution by x-ray diffraction in single crystals (*6*) and by NMR in solution (*7*). The same molecular architecture with five α helices was observed in the crystals and in solution, and in both states the carboxyl-terminal peptide of residues 64 to 69 was found to be unstructured. Initial studies of urea denaturation showed that the native, folded form and an unfolded form coexist over a wide range of urea concentrations at pH 4.8 and 18°C (*8*). In the absence of urea, only the NMR spectrum of the folded protein is seen. In 4.2 M urea, the two forms are present in equal concentrations and have an exchange life time of ~1 s. In 7 M urea,

Institut für Molekularbiologie und Biophysik, ETH-Hönggerberg, CH-8093 Zürich, Switzerland.

*Present address: Cambridge Centre for Protein Engineering, Hills Road, Cambridge CB2 2QII, United Kingdom.

†To whom correspondence should be addressed.

only the NMR spectrum of the unfolded form is seen. Sequence-specific NMR assignments for the urea-unfolded 434 repressor(1-69) showed significant deviations of some ^{1}H NMR chemical shifts from the random-coil values (9), indicating the presence of residual nonrandom structure (8). Combination of the chemical shift data with observations on slowed backbone amide proton exchange with the solvent then led to the conclusion that the nonrandom structure was located in the polypeptide segment 45 to 60, whereas for the remainder of the polypeptide chain a nonglobular flexible form was implicated.

For further characterization of the residual nonrandom structure in the urea-unfolded protein, we cloned a new polypeptide consisting of the amino-N-terminal 63 residues of the 434-repressor, and overexpressed it with uniform ^{15}N labeling and with selective ^{13}C labeling of the methyl groups of Val and Leu. By proteolytic cleavage of the 434-repressor(1-63), we further prepared the identically isotope-labeled polypeptide 434-repressor(44-63). The previously described (*10*) sequence-specific NMR assignments showed that the ^{1}H chemical shift deviations from the random coil values (9) observed in 434-repressor(1-69) are also present in both of these shorter polypeptides. Moreover, identical behavior at variable urea concentrations as described above for the 434-repressor(1-69) was observed for the 434-repressor(1-63). We used heteronuclear editing of ^{1}H nuclear Overhauser exchange spectroscopy (NOESY) spectra recorded with the ^{15}N- and ^{13}C-labeled polypeptides (*11–15*) to collect a set of NOE distance constraints (Fig. 1) and found a sufficiently high density of constraints for the polypeptide segment 53 to 60 to warrant a structure calculation (Fig. 2).

The input data used for the structure calculation (Fig. 1) are detailed in Table 1. An upper limit of 5.0 Å was attributed to all observable NOEs (Table 1) except for two intraresidual NOEs in Leu^{59} and Leu^{60}, for which a limit of 3.0 Å was determined from comparison with NOEs between vicinal protons and between the two methyl groups in the same residues. This procedure is in line with our long-standing practice of estimating NOE distance constraints involving peripheral amino acid side chain protons by using the uniform averaging model to account for time variations of the proton-proton distances due to internal mobility of the protein (*3, 16*). A more quantitative evaluation of the distance constraints was not warranted, considering that the data were collected from different spectra with different labeling of the heavy atoms (see legend to Fig. 1 for details). The usual correction of 1.0 Å was added to the upper distance limits when pseudoatoms were used to represent a methyl or methylene group (*17*). Five hundred calculations with the program DIANA (*18*) were started with random polypeptide conformations, and the 20 resulting conformers with the lowest residual target function values were further refined with the program AMBER (*19*) by using restrained energy minimization (*20*). These 20 energy-minimized DIANA conformers are used to represent the solution structure (Fig. 2). They contain no violations of NOE upper distance limits by more than 0.32 Å or of van der Waals constraints by more than 0.19 Å.

The result of the above structure determination with 434-repressor(1-63) shows that the polypeptide backbone of residues 54 to 59 and the orientations of the side chains of Val^{54}, Val^{56}, Trp^{58}, and Leu^{59} are well defined, with the isopropyl groups of all these Val and Leu residues in contact with the indole ring of Trp^{58} (Fig. 2). On the surface of the hydrophobic cluster formed by the side chains of residues 54, 56, 58, and 59, the hydrophilic side chains of Ser^{55} and Asp^{57} point toward the solvent and are disordered, and the backbone carbonyl oxygens also show a tendency of pointing outward toward the solvent. This visual impression of a well-defined local structure is confirmed by the root-mean-square deviations (RMSDs) of 0.74 Å for the backbone atoms of residues 54 to 59 and 1.07 Å for the backbone and the four hydrophobic side chains (Table 2). Moreover, the notion that Fig. 2 represents a meaningful structure determination for the urea-unfolded protein is supported by comparison with a corresponding group of 20 conformers calculated with identical techniques but without use of any NOE upper distance constraints in the input. These conformers have much larger RMSD values of 2.08 Å for the backbone atoms which increases to 3.39 Å when the hydrophobic side chains are included (Table 2). As an additional reference, Table 2 shows also that the same polypeptide segment has significantly smaller RMSD values in the NMR structure of the native 434 repres-

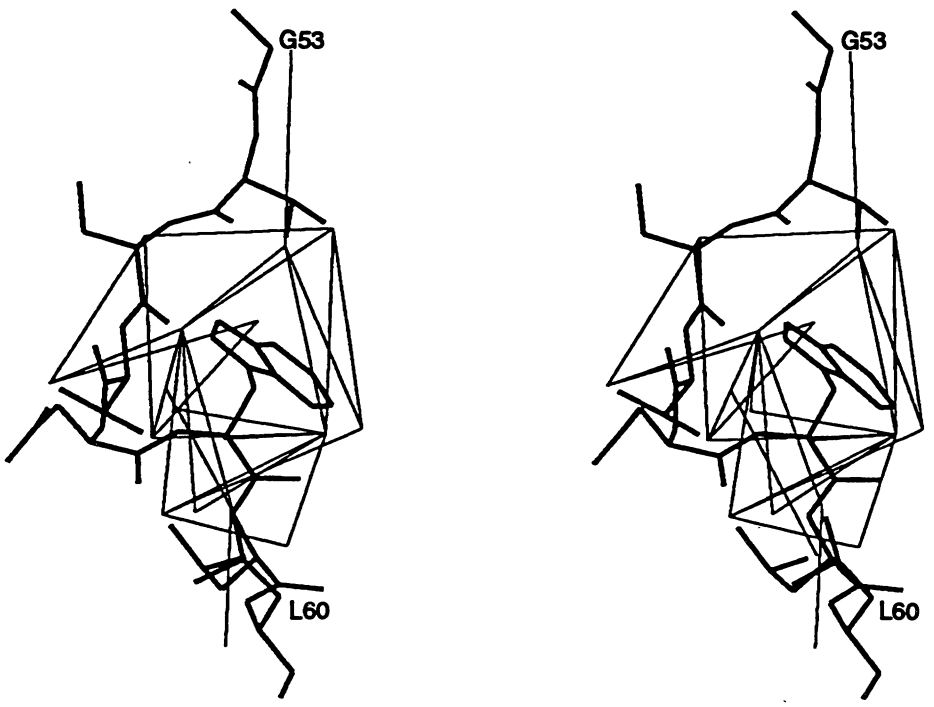

Fig. 1. Survey of the NMR constraints used as input for the presently reported structure determination. The figure shows an all–heavy-atom stereo view of one of the conformers of the polypeptide segment 53 to 60 from 434-repressor shown in Fig. 2, which were calculated from NMR data measured in 7 M aqueous urea solutions of 434-repressor(1-63) and 434-repressor(44-63) at pH 4.8 and 18°C (*25*). Thin lines connect those pairs of hydrogen atom positions [or pseudoatom positions representing the methyl groups (*17*)] for which a NOE distance constraint was measured and used in the input for the structure calculation. The NOEs were collected from five two-dimensional NMR spectra: heteronuclear-resolved ^{13}C(ω_2)-half-filter ^{1}H,^{1}H-NOESY (*15*) with the two protein fragments enriched with ^{13}C at the Val and Leu methyl positions; NOE-relayed ^{15}N,^{1}H-COSY (*26*) with the two uniformly ^{15}N-labeled polypeptides; and ^{1}H,^{1}H-NOESY of the unlabeled 434-repressor(44-63). A mixing time of 300 ms was used, which was sufficiently short to avoid significant spin diffusion, as evidenced by the following controls: (i) for the indole NH proton of Trp^{58}, Nε^1H, intraring NOEs were observed only to δ^1H and ζ^2H; (ii) the NOE buildup curves were to a good approximation linear for mixing times in the range from 0 to 450 ms; and (iii) in the Leu residues, largely different NOE intensities were observed between the α proton and the δ^1 or δ^2 methyl group, respectively.

sor(1-69), which was obtained at high quality from a carefully quantitated input of NOE distance constraints and dihedral-angle constraints (*7*).

The approach used for the structure determination in Fig. 2 was based on the fact that the NMR spectrum at 7 M urea contains only one resonance line for each proton (*8*, *10*), which shows that all protein conformations present in this solution are in rapid exchange on the chemical-shift time scale (*3*). Because a quantitative evaluation of the NOE intensities was not warranted (see above) and in particular no absolute NOE intensities were obtained, the NOE data provide no direct evidence for the extent of the population of the structure shown in Fig. 2, except that the NOESY cross peaks would be undetectably weak if the population of the folded conformation were less than ~10%. However, the observation that the data of Table 1 can be satisfied by a single, quite well-defined structure (Fig. 2 and Table 2) implies that whatever the population of this structure is, all other conformations present in the solution do not significantly contribute to the NOEs in Table 1. In other words, because the NOE intensity decreases with the inverse sixth power of the distance between two protons (*3*), the molecular conformations in which a given ^1H-^1H distance exceeds 5.0 Å do not contribute to the overall intensity of the corresponding NOE. This averaging is in contrast to the observed chemical shifts, which represent an average of the chemical shifts in all conformations present and the contribution from each molecular species is simply weighted by its population in the solution studied. This different averaging of NOE intensities and chemical shifts (*21*) is manifest in the result of the present structure determination: Although the previously reported deviations of the ^1H chemical shifts in the polypeptide segment 53 to 60 from the random coil values (*8*, *10*) can be qualitatively rationalized by the close approach of the aliphatic side chains to the indole ring of Trp^{58} (Fig. 2), ring current calculations for the methyl protons in the structure of Fig. 2 predict larger deviations from the random-coil shifts (9) than those observed (*8*, *10*), with the largest discrepancies for γ^2CH_3 of Val^{54}, γ^1CH_3 of Val^{56}, and δ^2CH_3 of Leu^{59}. This result indicates that the observed chemical shifts include important contributions from fully unfolded polypeptides with random coil shifts. On this basis, the chemical shift measurements provide presently the most direct indication that in 7 M urea solution the structure of Fig. 2 is present in an equilibrium with conformers that do not contain a compact structure involving the residues 54 to 59.

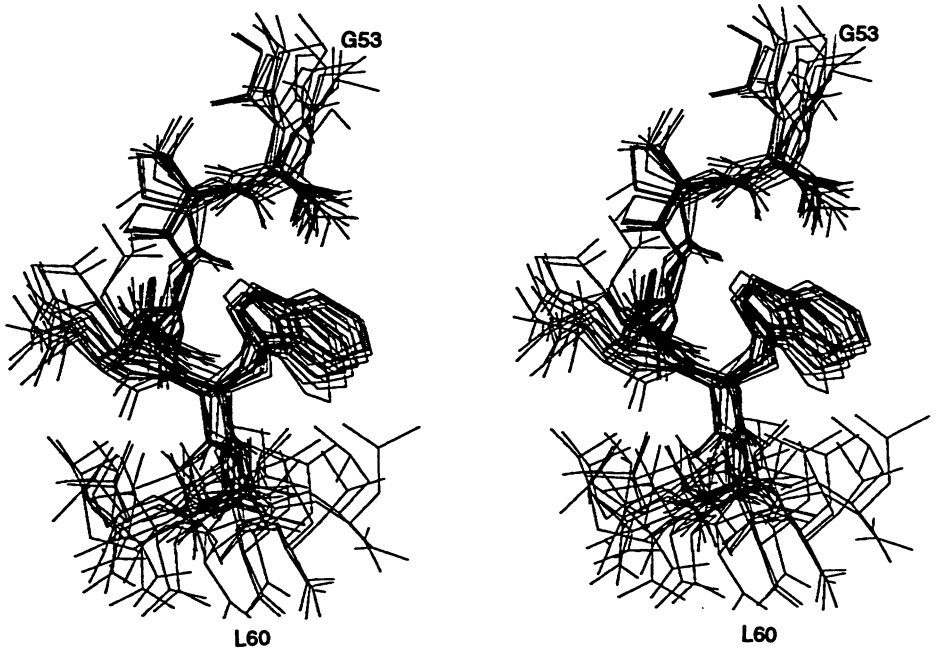

Fig. 2. Result of the structure calculations from the input data of Table 1 for the polypeptide segment Gly^{53}-Val-Ser-Val-Asp-Trp-Leu-Leu^{60} of the 434-repressor(1-63) unfolded in 7 M urea at pH 4.8 and 18°C. The figure shows an all–heavy-atom stereo view of the 20 conformers selected to represent the solution structure. The conformers 2 through 20 were superimposed with conformer 1 for minimal RMSD of the backbone atoms of residues 54 to 59.

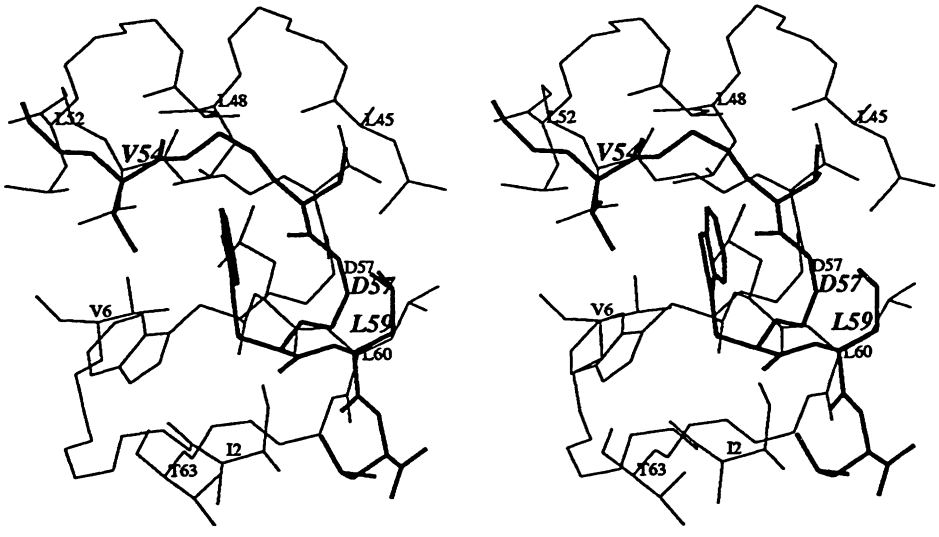

Fig. 3. Stereo view of the all–heavy-atom presentation of one of the conformers from Fig. 2 of the segment Gly^{53}-Val-Ser-Val-Asp-Trp-Leu-Leu^{60} in the urea-unfolded 434-repressor(1-63) (thick lines, bold labels) superimposed with fragments of the native solution structure of the 434-repressor(1-69) (*7*) (thin lines, small labels). The two structures were superimposed for optimal fit of the backbone atoms of residues 54 to 57. For the native structure, the backbone is drawn for the residues 2 to 6 and 45 to 63 and the side chains are included for Ile^2, Val^6, Leu^{45}, Leu^{48}, Ala^{49}, Leu^{52}, residues 53 to 60, and Thr ^{63}.

The structure of residues 54 to 59 in urea-unfolded 434-repressor are compared with the corresponding peptide segment in the folded protein (*6*, *7*) in Fig. 3. In the two species, a similar loop is formed by the backbone atoms of residues 54 to 57 and the side chains of Val^{54} and Val^{56} are in nearly identical locations. Because of the formation of helix 5 in the native structure, the indole ring of Trp^{58} in the hydrophobic cluster formed with residues 54, 56, and 59 in the unfolded form is replaced by the side chain of Leu^{59}, the space of which is in turn occupied by Leu^{60}. In this way the hydrophobic cluster observed in the urea-unfolded form is essentially preserved in the folded protein. Similarity of the folded and urea-unfolded forms of the 434-repressor in the region of residues 54 to 59 is also evidenced

by the fact that the RMSD values between these two structures are less than those between the urea-unfolded protein and a randomized form, especially when the hydrophobic side chains are included (Table 2). Figure 3 shows further that the polypeptide fold in the globular form of the 434-repressor(1-69) (6, 7) brings the side chains of Val^{54}, Val^{56}, Leu^{59}, and Leu^{60} in contact with the apolar residues Ile^{2}, Val^{6}, Leu^{45}, Leu^{48}, Ala^{49}, and Leu^{52}. The local hydrophobic cluster relating to that seen in the urea-unfolded form of the protein is thus expanded to a global hydrophobic core by interactions of residues that are further apart in the amino acid sequence. Such longer range interactions also ensure the formation of a predominantly hydrophobic environment for Trp^{58} in the folded protein.

From the experience gained with the presently described project, two conclusions can be drawn relating to NMR experiments that are frequently used with proteins. First, the importance of having obtained individual, stereospecific assignments for all methyl resonances of Val and Leu (8, 10) cannot be overemphasized. Otherwise, the hydrophobic cluster formed by residues 54, 56, 58, and 59 could hardly have been characterized. For unfolded forms of proteins these stereospecific assignments can in practice only be obtained by using the method of biosynthetically directed fractional ^{13}C labeling (22). Second, considering that the 434-repressor(1-63) is a protein devoid of disulfide bonds or prosthetic groups that might stabilize residual local structure (5), the observation of nonrandom structure in 7 M urea implies that it may be difficult with certain proteins to prepare a fully random reference state, for example, for the analysis of amide proton exchange measurements during refolding (23). Extreme care should be exercised to distinguish between experimental manifestations of such residual local structure in the denatured reference state and manifestations of the formation of folding intermediates after initiation of the refolding process.

Finally, it is tempting to speculate on possible folding pathways starting from the polypeptide conformation observed in 7 M urea, that is, an ensemble of nonglobular flexible forms of the polypeptide chain including a sizeable population of conformers containing a local nonrandom hydrophobic cluster. Figure 4 illustrates that the polypeptide chain in the folded, globular state of the 434-repressor(1-63) (6, 7) forms two subdomains containing, respectively, the helices 1 to 3 (residues 1 to 36) and the helices 4 and 5 (residues 45 to 60). The two subdomains are covalently linked by a somewhat flexible loop (7). Formation of this structure could be initiated by the strictly localized "nucleation cluster" with the side chains of residues 54, 56, 58, and 59 (Fig. 2). In a subsequent step, the helix 57 to 60 would be formed, resulting in the replacements of Trp^{58} by Leu^{59} and of Leu^{59} by Leu^{60} in the nucleation cluster (Fig. 3). As another event following the

Table 1. Input for the calculation of the residual structure of the fragment 53 to 60 in the 434-repressor(1-63) dissolved in water containing 7 M urea at pH = 4.8 and 18°C.

NOE distance constraints		
Atom 1*	Atom 2*	Upper limit [Å]†
Gly^{53} αCH_2	Val^{54} γ^2CH_3	7.0
Val^{54} γ^1CH_3	Ser^{55} αH	6.0
Val^{54} γ^1CH_3	Trp^{58} ζ^3H	6.0
Val^{54} γ^1CH_3	Trp^{58} ϵ^3H	6.0
Val^{54} γ^1CH_3	Trp^{58} δ^1H	6.0
Val^{54} γ^2CH_3	Trp^{58} ζ^3H	6.0
Val^{54} γ^2CH_3	Trp^{58} ϵ^3H	6.0
Val^{54} γ^2CH_3	Trp^{58} δ^1H	6.0
Ser^{55} αH	Val^{56} γ^1CH_3	6.0
Ser^{55} αH	Val^{56} γ^2CH_3	6.0
Val^{56} γ^1CH_3	Trp^{58} ζ^2H	6.0
Val^{56} γ^1CH_3	Trp^{58} ϵ^3H	6.0
Val^{56} γ^1CH_3	Trp^{58} δ^1H	6.0
Val^{56} γ^2CH_3	Trp^{58} ζ^2H	6.0
Val^{56} γ^2CH_3	Trp^{58} δ^1H	6.0
Val^{56} αH	Leu^{59} δ^1CH_3	6.0
Trp^{58} HN	Trp^{58} ϵ^3H	5.0
Trp^{58} HN	Trp^{58} δ^1H	5.0
Trp^{58} αH	Trp^{58} ϵ^3H	5.0
Trp^{58} δ^1H	Leu^{59} δ^2CH_3	6.0
Trp^{58} ϵ^3H	Leu^{59} HN	5.0
Trp^{58} δ^1H	Leu^{59} HN	5.0
Trp^{58} ϵ^3H	Leu^{59} αH	5.0
Trp^{58} ζ^3H	Leu^{59} δ^2CH_3	6.0
Trp^{58} ϵ^3H	Leu^{59} δ^2CH_3	6.0
Trp^{58} δ^1H	Leu^{60} δ^2CH_3	6.0
Leu^{59} αH	Leu^{59} δ^2CH_3	4.0
Leu^{60} αH	Leu^{60} δ^2CH_3	4.0

*These two columns identify the pairs of protons for which an NOE has been observed. The protons are identified by the three-letter amino acid code, the sequence position, and the location in the amino acid residue in the standard IUB-IUPAC nomenclature. †Upper limit to the proton-proton distance after correction for use of pseudoatoms to represent methylene and methyl groups (17). The lower limit was set equal to the sum of the van der Waals radii.

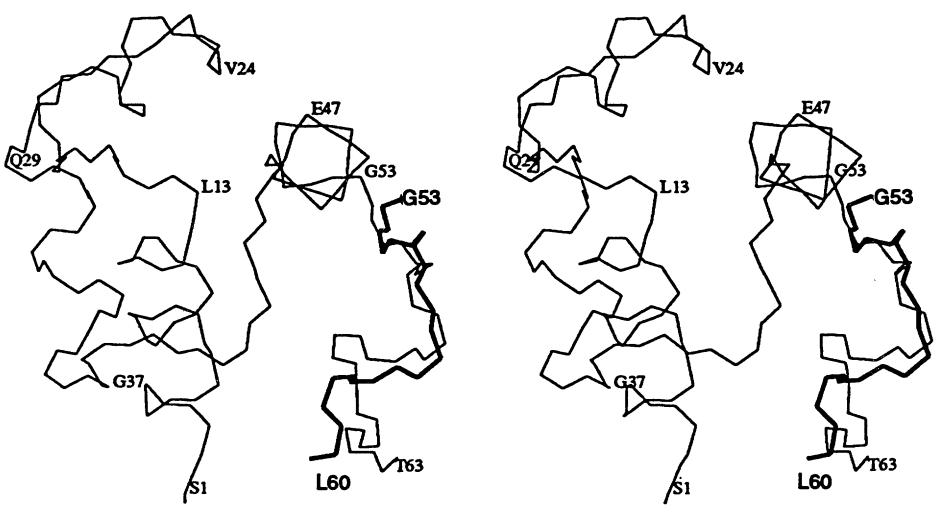

Fig. 4. Stereo view of the polypeptide backbone for the segment 1 to 63 in the NMR solution structure of native 434-repressor(1-69) (thin line, small labels) (7). Also drawn with a thick line and bold labels is the backbone of the segment 53 to 60 of the urea-unfolded 434-repressor(1-63). The two structures were superimposed for optimal fit of the backbone atoms of residues 54 to 57.

Table 2. Comparisons of the polypeptide segment 53 to 60 in the urea-unfolded 434-repressor(1-63) with the corresponding segment in native 434-repressor(1-69) and in a hypothetical random-coil form.

Atoms compared*	RMSD (Å)				
	⟨Urea⟩†	⟨Random⟩‡	⟨Native⟩§	⟨Urea⟩-⟨native⟩‖	⟨Urea⟩-⟨random⟩¶
Backbone of residues 54 to 59	0.74	2.08	0.17	1.67	2.01
Same + side chains of 54, 56, 58, and 59	1.07	3.39	0.31	2.80	4.13

*The backbone atoms used for calculating the RMSDs are N, Cα, and C′. †Group of 20 energy-minimized DIANA conformers used to represent the solution structure in 7 M urea. This column lists the average of the pairwise RMSDs in this group of conformers. ‡Group of 20 energy-minimized DIANA conformers calculated with identical procedures as ⟨urea⟩ and ⟨native⟩, except that no NOE upper distance constraints were used. This column lists the average of the pairwise RMSDs in this group of conformers. §Group of 20 energy-minimized DIANA conformers representing the native solution structure of 434-repressor(1-69) (7). This column lists the average of the pairwise RMSDs in this group of conformers. ‖Average of the pairwise RMSDs for all combinations of conformers in ⟨urea⟩ with those in ⟨native⟩. ¶Average of the pairwise RMSDs for all combinations of conformers in ⟨urea⟩ with those in ⟨random⟩.

folding of the nucleation cluster, formation of the helix 4 would induce a "hydrophobic collapse" (*24*) in the subdomain on the right of Fig. 4, resulting in a more extensive hydrophobic core around the nucleation cluster (Fig. 3). In further steps, hydrophobic contacts with the first subdomain mediated by the apolar side chains of Leu^{48}, Leu^{52}, and Leu^{59} would lead to further growth of the hydrophobic core and proper spatial positioning of the two subdomains (Fig. 4). Although this selection of distinct folding events derived from combined inspection of the structures of folded and urea-unfolded 434-repressor(1-63) is largely hypothetical, it may provide a platform for additional experiments to investigate spatial and temporal patterns of the order in which distinct, individual folding events take place.

REFERENCES AND NOTES

1. F. M. Richards, *Sci. Am.* **264**, 54 (January 1991).
2. C. M. Dobson, *Curr. Opin. Struct. Biol.* **1**, 22 (1991).
3. K. Wüthrich, *NMR of Proteins and Nucleic Acids* (Wiley, New York, 1986).
4. ———, *Science* **243**, 45 (1989).
5. J. Anderson, M. Ptashne, S. C. Harrison, *Proc. Natl. Acad. Sci. U.S.A.* **81**, 1307 (1984).
6. A. Mondragon, S. Subbiah, S. C. Almo, M. Drottar, S. C. Harrison, *J. Mol. Biol.* **205**, 189 (1989).
7. D. Neri, M. Billeter, K. Wüthrich, *ibid.* **223**, 743 (1992).
8. D. Neri, G. Wider, K. Wüthrich, *Proc. Natl. Acad. Sci. U.S.A.* **89**, 4397 (1992).
9. A. Bundi and K. Wüthrich, *Biopolymers* **18**, 285 (1979).
10. D. Neri, G. Wider, K. Wüthrich, *FEBS Lett.* **303**, 129 (1992).
11. G. Otting, H. Senn, G. Wagner, K. Wüthrich, *J. Magn. Reson.* **70**, 500 (1986).
12. S. W. Fesik, *Nature* **332**, 865 (1988).
13. R. H. Griffey and A. G. Redfield, *Q. Rev. Biophys.* **19**, 51 (1987).
14. G. Otting and K. Wüthrich, *ibid.* **23**, 39 (1990).
15. G. Wider, C. Weber, K. Wüthrich, *J. Am. Chem. Soc.* **113**, 4676 (1991).
16. W. Braun, Ch. Bösch, L. R. Brown, N. Gō, K. Wüthrich, *Biochim. Biophys. Acta* **667**, 377 (1981).
17. K. Wüthrich, M. Billeter, W. Braun, *J. Mol. Biol.* **169**, 949 (1983).
18. P. Güntert, W. Braun, K. Wüthrich, *ibid.* **217**, 517 (1991).
19. U. C. Singh, P. K. Weiner, J. W. Caldwell, P. A. Kollman, *AMBER 3.0* (University of California, San Francisco, 1986).
20. M. Billeter, Th. Schaumann, W. Braun, K. Wüthrich, *Biopolymers* **29**, 695 (1990).
21. In this context, one should also recall that only a short lifetime of ~1 ns is needed for a protein conformation to give rise to negative NOEs [G. Otting, E. Liepinish, K. Wüthrich, *Science* **254**, 974 (1991)], as observed in the urea-unfolded 434-repressor(1-63) and 434-repressor(44-64). In contrast, chemical shift averaging is typically observed between different conformers even when they have a life time of the order of 1 ms.
22. H. Senn *et al.*, *FEBS Lett.* **249**, 113 (1989); D. Neri, Th. Szyperski, G. Otting, H. Senn, K. Wüthrich, *Biochemistry* **28**, 7510 (1989).
23. H. Roder and K. Wüthrich, *Proteins* **1**, 34 (1986); H. Roder, G. A. Elove, S. W. Englander, *Nature* **335**, 700 (1988); J. B. Udgaonkar and R. L. Baldwin, *ibid.*, p. 694.
24. H. S. Chan and K. A. Dill, *Proc. Natl. Acad. Sci. U.S.A.* **87**, 6388 (1990).
25. Abbreviations for the amino acid residues are: A, Ala; C, Cys; D, Asp; E, Glu; F, Phe; G, Gly; H, His; I, Ile; K, Lys; L, Leu; M, Met; N, Asn; P, Pro; Q, Gln; R, Arg; S, Ser; T, Thr; V, Val; W, Trp; and Y, Tyr.
26. G. Otting and K. Wüthrich, *J. Magn. Reson.* **76**, 569 (1988).

27. Supported by the Schweizerischer Nationalfonds (project no. 31.25174.88). We thank R. Marani for the careful processing of the manuscript.

1 May 1992; accepted 15 July 1992

Attention-Based Motion Perception

Patrick Cavanagh

Two "attentive" tracking tasks reveal the existence of an attention-based motion process. In the first task, oppositely rotating luminance and color gratings were superimposed. Because of masking from the color grating, the bars of the luminance grating were not visible; nevertheless, their motion was visible and it determined the perceived direction of the stimulus rotation. On the other hand, the bars of the color grating were visible but they could only be seen to move (in the opposite direction to the overall stimulus rotation) when they were tracked with attention. In a second task, the perceived velocity of a color grating, typically slow at equiluminance, speeded up when individual bars were attentively tracked. These findings demonstrate two independent motion processes: one that is "low-level" or automatic in that it signals motion even in the absence of attention to the stimulus, and one that is mediated by attention to visible features and provides accurate velocity judgments independently of the features being tracked.

Attention often plays a crucial role in motion perception. For example, when a stimulus contains two components moving in opposite directions, attentive tracking of either one can reveal its motion independently of the other (*1*, *2*). Many neurons in primary visual cortex are sensitive to the direction of motion (*3*) and attention might act by selecting one or the other of these low-level motion responses. However, the experiments described here demonstrate that the perception of motion during attentive tracking can arise independently of low-level motion responses and may be derived from the internal signals that move the focus of attention (*4*).

In the first experiment, the stimulus was constructed by superimposing color and luminance gratings that moved in opposite directions around an annulus (Fig. 1A) in order to eliminate the possibility of tracking eye movements (*5*). Measurements of detection and motion thresholds, motion strength, and tracking performance were made. An unexpected feature of the results is that the superimposed color grating greatly increased the separation between the pattern and motion thresholds (*6*) for the luminance grating. Without the superimposed color grating, the thresholds for seeing the luminance component and seeing it move were very close, replicating earlier findings (*7*). With the superimposed color grating, both detection and direction thresholds rose by a factor of 4 or 5, again replicating earlier findings (*8*). However, as will be seen, an additional order of magnitude of contrast was necessary before the luminance grating could be tracked, implying that the features that mediated the detection of the grating and its motion do not support its localization or tracking.

The relative strengths of the color and luminance contributions to the apparent global rotation of the combined stimulus were determined with a nulling procedure. The color contrast was set at 40% of the maximum available contrast between the red and green phosphors (*9*), and the relative modulations of red and green were set to approximate equiluminance with the use of a minimum apparent speed criterion (*10*). The observers then adjusted the contrast of the luminance grating to null the global motion seen in the annulus without paying attention to the individual features of the two gratings. At low values of luminance contrast, the combined stimulus appeared as a red-green grating rotating smoothly in the direction of the color component. At high values of luminance contrast, the stimulus appeared to be a flickering red-green grating rotating with a jerky motion in the direction of the luminance grating. At some intermediate value between 5 to 10% contrast (depending on the observer), the global motion was nulled and its direction became ambiguous.

The same combined stimulus was used in the tracking task; however, the contrast of the luminance grating was set to one of eight values uniformly spaced from 5% to an upper value of 25 to 45% (*11*), whereas the color contrast remained fixed at 40%. For each trial, the observer carefully fixated the central bull's-eye. To begin the trial, an inner pointer appeared beside the pair of

Department of Psychology, Harvard University, Cambridge, MA 02138.